Arabian Journal of Chemistry (2022) **15**, 104203

King Saud University

Arabian Journal of Chemistry

www.ksu.edu.sa
www.sciencedirect.com

ORIGINAL ARTICLE

Euphorane C, an unusual C17-norabietane diterpenoid from *Euphorbia dracunculoides* induces cell cycle arrest and apoptosis in human leukemia K562 cells

Xue-Long Yan [a,b], Ming-Feng Zou [c], Bei-Ling Chen [a], Fang-Yu Yuan [c], Qin-Feng Zhu [a], Xu Zhang [a], Yan Lin [a], Qing-De Long [a], Wu-Ling Liu [a,*], Shang-Gao Liao [a,*]

[a] *State Key Laboratory of Functions and Applications of Medicinal Plants & School of Pharmacy, Guizhou Medical University, Guian New District 550025, Guizhou, China*
[b] *School of Basic Medical Sciences, Guizhou Medical University, Guian New District 550025, Guizhou, China*
[c] *School of Pharmaceutical Sciences, Sun Yat-sen University, Guangzhou, 510006, Guangdong, China*

Received 20 July 2022; accepted 14 August 2022
Available online 19 August 2022

KEYWORDS

Euphorbia dracunculoides;
Cytotoxicity;
Apoptosis;
Abietane diterpenoid;
Norabietane

Abstract Four new polycyclic diterpenoids euphoranes A − D (**1**–**4**), together with 12 known terpenoids (**5**–**16**) were isolated from the whole plants of *Euphorbia dracunculoides*. Compound **2** represents the first example of aromatic 15,16,17-trinorabietane diterpenoid in *Euphorbia* species, and euphorane C (**3**) is an unusual 17-norabietane diterpenoid. The absolute configurations of **1**, **2**, and **4** were determined by single crystal X-ray diffraction, while that of **3** was established with the aid of ECD and 1D NMR quantum chemical calculation. Moreover, the absolute stereochemistry of **11** was demonstrated for the first time by crystallographic data. Compounds **1**–**16** were screened for antiproliferative activities against five human cancer cell lines, and **3** showed significant cytotoxicity against the human leukemia K562 cells with IC_{50} value of 3.59 μM. Preliminary mechanistic investigation revealed that **3** could induce cell cycle arrest at G0/G1 phase and apoptosis in K562 cells.

* Corresponding authors.
E-mail addresses: emmalao@163.com (W.-L. Liu), lshangg@163.com (S.-G. Liao).
Peer review under responsibility of King Saud University.

Production and hosting by Elsevier

https://doi.org/10.1016/j.arabjc.2022.104203
1878-5352

1. Introduction

Natural products are important sources of "privileged structures" in drug development (Cragg et al., 2009). For anti-cancer agents, about 70 % of FDA-approved antitumor drugs are either natural products or their derivatives (Newman et al., 2020). Among them, the nonspecific "higher diterpenes" (also known as polycyclic diterpenoids) with a common 6/6/6 ring system from *Euphorbia* species are of particular significance due to their extensive physiological activities. Polycyclic diterpenoids are well-known for their structural diversity with many different skeletal types, such as rosanes, abietanes, atisanes, and kauranes (Shi et al., 2008; Vasas et al., 2014; Xu et al., 2021). Abietane diterpenoids from *Euphorbia* are usually substituted by an α,β-unsaturated γ-lactone ring at C-12 and C-13. Kauranes comprise a perhydrophenanthrene unit (A, B, and C rings) fused with a cyclopentane (D ring), while in atisanes, the perhydrophenanthrene unit is fused with a cyclohexane (Vasas et al., 2014). Recent studies have shown that polycyclic diterpenoids may be potential chemical entities in future antitumor drug development. For example, jolkinolide B, an abietane diterpene, could induce apoptosis and sensitize bladder cancer to mTOR inhibitors (Sang et al., 2021; Sang et al., 2022). 8,9-Seco-*ent*-kaurene, a kaurane diterpene, could effectively suppress triple-negative breast cancer cells *via* Akt signaling pathway (Fan et al., 2021).

Euphorbia dracunculoides, a perennial herb of the genus *Euphorbia*, is mainly distributed in North Africa, South Europe, and Southwest Asia (Wang et al., 2015a). Previous phytochemical studies showed that the plant is rich in diterpenes with different skeletal types, such as lathyranes, myrsinanes, and tiglianes, etc. (Chi et al., 2016; Dai et al., 2016; Wang et al., 2015a, 2015b, 2016, 2017). In our ongoing efforts to discover antitumor diterpenoids from *Euphorbia* plants (Chen et al., 2022; Yan et al., 2019), four new polycyclic diterpenoids (**1**–**4**) and 12 known compounds were isolated from the EtOAc fraction of *E. dracunculoides*. Compounds **2** and **3** represent unusual examples of aromatic abietane norditerpenoids in *Euphorbia* species. All the compounds were tested for antiproliferative activities against five human cancer cell lines, and **3** showed significant activity against the human leukemia K562 cells with micromolar IC_{50}. Herein, we reported the isolation, structural identification, and cytotoxicity of these compounds.

2. Material and methods

2.1. General information

Optical rotations were tested on a Rudolph Autopol I automatic polarimeter. UV spectra were tested on a Shimadzu UV-2450 spectrophotometer, and IR spectra were recorded on Bruker Tensor 37 infrared spectrophotometers. ECD spectra were measured on an Applied Photophysics Chirascan spectrometer. NMR data were measured on Bruker AM-400/500 spectrometers at 25 °C. HRESIMS was performed on a Waters Micromass Q-TOF spectrometer. Column chromatography (CC) was performed on silica gel (Particle size 37–48 μm, Qingdao Haiyang Chemical Co., ltd.), reversed-phase C_{18} (RP-C_{18}) (S-50 μm, 12 nm, YMC Co., ltd.), D101 macroreticular resin (Polystyrene, non-polar, particle size 0.315–0.7 mm, pore diameter 9–15 nm, surface area 500–550 m^2/g, Donghong Chemical Co., ltd.), and Sephadex LH-20 gel (Amersham Biosciences). A Shimadzu LC-20 AT equipped with a SPD-M20A PDA detector was used for HPLC. An YMC-pack ODS-A column (250 × 10 mm, S-5 μm, 12 nm) was used for semi-preparative HPLC separation. All solvents were analytical grade (Guangzhou Chemical Reagents Company, ltd.).

2.2. Plant material

The whole plant of *Euphorbia dracunculoides* Lam. (Euphorbiaceae) were collected in July 2020 from Dali city, Yunnan Province, China and identified by one of the authors, Qing-De Long. A voucher specimen (number: HZDJ202007) was deposited at the School of Pharmacy, Guizhou Medical University.

2.3. Extraction and isolation

The air-dried powder of *E. dracunculoides* (20 kg) was extracted with 95 % EtOH (3 × 50 L) at room temperature to give a crude extract (3 kg), which was suspended in H_2O (3 L) and then partitioned with EtOAc. The resulting EtOAc extract (800 g) was subjected to D101 macroreticular resin eluted with a MeOH/H_2O gradient (30:70 → 100:0) to afford four fractions (Fr. I – Fr. IV). Fr. II was separated by silica gel chromatographic column (CC) (CH_2Cl_2/MeOH, 200:1 → 10:1) to give three fractions (Fr. IIa – Fr. IIc). Fr. IIc was recrystallized in MeOH to yield **8** (1.03 g). Fr. III was subjected to silica gel CC eluted with a petroleum ether (PE)/EtOAc gradient (10:1 → 1:3) to give three fractions (Fr. IIIa – Fr. IIIc). Fr. IIIa was separated by RP-C_{18} silica gel CC eluted with MeOH/H_2O (50:50 → 100:0) to give Fr. IIIa1 and Fr. IIIa2. Fr. IIIa2 was separated by Sephadex LH-20 (MeOH), followed by semipreparative HPLC (MeCN/H_2O, 70:30, 3 mL/min) to afford **15** (11 mg, t_R 8.4 min) and **11** (31 mg, t_R 7.3 min). Fr. IIIc was separated by Sephadex LH-20 (MeOH) followed by semipreparative HPLC (MeCN/H_2O, 75:25, 3 mL/min) to give **12** (8 mg, t_R 12.3 min), **14** (9 mg, t_R 14.1 min), and **16** (10 mg, t_R 14.5 min). Fr. IV (140 g) was separated by silica gel CC (PE/EtOAc) to give five fractions (Fr. IVa – Fr. IVe). Fr. IVa was separated by RP-C_{18} silica gel CC followed by HPLC (MeCN/H_2O, 75:25, 3 mL/min) to yield **1** (38 mg, t_R 14.5 min) and **13** (5 mg, t_R 10.1 min). Fr. IVb was separated by RP-C_{18} silica gel CC (MeOH/H_2O, 60:40 → 90:10) to give Fr. IVb1 and Fr. IVb2. Fr. IVb1 was purified by HPLC (MeCN/H_2O, 90:10, 3 mL/min) to give **3** (30 mg, t_R 12.0 min). Fr. IVb2 was purified by HPLC (MeCN/H_2O, 70:30, 3 mL/min) to afford **2** (24 mg, t_R 13.3 min) and **7** (20 mg, t_R 16.0 min). Fr. IVd was separated by silica gel CC to give Fr. IVd1 and Fr. IVd2. Fr. IVd1 was separated by HPLC (MeCN/H_2O, 80:20, 3 mL/min) to give **4** (11 mg, t_R 11.8 min) and **5** (5 mg, t_R 8.1 min). Fr. IVd2 was purified by HPLC (MeCN/H_2O, 70:30, 3 mL/min) to afford **6** (15 mg, t_R 12.1 min). Fr. IVe was separated by silica gel CC (CH_2Cl_2/MeOH, 200:1 → 10:1), Sephadex LH-20 (MeOH), followed by HPLC (MeCN/H_2O, 80:20, 3 mL/min) to afford **10** (8 mg, t_R 15.5 min) and **9** (10 mg, t_R 12.5 min).

2.3.1. 14β-Hydroxy-ent-abieta-13(15)-ene-12α,16-olide (euphorane A) (1)

Colorless needles; mp 190.7–193.6 °C; $[\alpha]_D^{20}$ – 80.8 (*c* 0.28, MeOH); UV (MeCN) λ_{max} (log ε) 221 (4.13) nm; IR (KBr) ν_{max} 3421, 2924, 1742, 1684, 1476, 1366, 1261, 1226, 1088, 1034, 832, and 735 cm^{-1}; ^1H and ^{13}C NMR data see Tables 1 and 2, respectively; HRESIMS *m/z* 339.1920 $[M + Na]^+$ (calcd for $C_{20}H_{28}O_3Na$, 339.1931).

Table 1 ^{1}H NMR data of compounds **1**–**4** (400 MHz, J in Hz, δ in ppm).

Position	**1**[a]	**2**[b]	**3**[c]	**4**[c]
1	0.97, dd (13.1, 4.0)	β 1.32, m	β 1.35, m	0.96, m[d]
	1.83, m	α 2.18, dt, (13.3, 3.9)	α 2.08, d (12.2)	1.51, m
2	1.46, m[d]	1.58, m	1.45, m	1.82, m
	1.59, m	1.75, dt (13.3, 3.3)	1.62, m[d]	
3	1.17, m	1.22, m	1.13, ddd (17.0, 13.4, 3.7)	3.44, m
	1.45, m[d]	1.46, dt (13.1, 3.5)	1.37, m	
5	1.26, dd (12.1, 4.7)	1.25, m,	1.23, dd (12.9, 2.0)	0.82, m,
6	α 1.98, m	α 1.60, m	α 1.59, m[d]	1.53, m
	β 2.15, m	β 1.88, dd (13.1, 7.8)	β 1.86, dd (12.9, 8.0)	
7	5.99, s	α 2.75, dd (17.3, 6.0)	α 3.05, dd (17.5, 6.1)	α 2.47, dt (13.3, 3.2)
		β 2.43, ddd (17.3, 11.8, 7.8)	β 2.70, ddd (17.5, 11.7, 8.0)	β 0.88, m
8				
9	2.42, m			1.46, m
11	β 1.55, m[d]	6.25, d (2.3)	6.70, s	1.75, m
	α 2.29, ddd (13.5, 6.2, 2.8)			
12	4.58, dd (11.8, 6.2)			2.87, dd (6.2, 2.9)
13		6.10, d (2.3)		5.41, d (2.9)
14	5.05, s			
15				2.33, m
16			2.95, s	
17	1.97, s			4.88, dd (4.0, 2.3)
				5.05, dd (4.0, 2.3)
18	0.91, s	0.95, s	0.91, s	1.20, s
19	0.88, s	0.92, s	0.86, s	0.96, s
20	0.86, s	1.16, s	1.18, s	0.73, s

[a] Measured in $CDCl_3$
[b] Measured in CD_3OD.
[c] Measured in Pyrdine-d_5.
[d] overlapped.

Table 2 ^{13}C NMR data of compounds **1**–**4** (100 MHz, δ_C in ppm).

Position	**1**[a]	**2**[b]	**3**[c]	**4**[c]
1	38.7	40.3	39.0	37.0
2	18.5	20.4	19.9	28.1
3	42.1	42.9	42.1	78.4
4	32.8	34.4	34.0	39.6
5	49.5	51.7	50.3	55.0
6	23.7	19.8	19.2	19.6
7	129.6	25.1	24.6	31.7
8	135.8	114.7	115.1	48.4
9	44.1	153.3	159.8	51.9
10	36.2	38.9	39.0	38.4
11	27.0	103.3	102.9	26.0
12	78.3	156.4	160.1	44.2
13	123.7	100.3	109.3	75.6
14	70.5	156.4	163.1	212.6
15	162.3		205.9	43.9
16	174.9		33.9	143.9
17	9.1			110.6
18	33.0	33.8	33.7	29.3
19	21.8	22.1	22.2	16.8
20	13.1	25.2	24.7	14.3

[a] Measured in $CDCl_3$.
[b] Measured in CD_3OD.
[c] Measured in Pyrdine-d_5.

2.3.2. 12,14-Dihydroxy-15,16,17-trinorabieta-8,11,13-triene (euphorane B) (2)

Colorless crystals; mp 176.8–179.0 °C; $[\alpha]_D^{20}$ − 45 (*c* 1.5, MeOH); UV (MeCN) λ_{max} (log ε) 202 (3.63) nm; IR (KBr) ν_{max} 3306, 2925, 1593, 1456, 1310, 1132, 1041, 1012, and 838 cm^{-1}; ^1H and ^{13}C NMR data see Tables 1 and 2, respectively; HRESIMS *m/z* 259.1707 $[M - H]^-$ (calcd for $C_{17}H_{23}O_2$, 259.1704).

2.3.3. 12,14-Dihydroxy-17-norabieta-8,11,13-triene-15-one (euphorane C) (3)

Yellowish oil; $[\alpha]_D^{20}$ − 40.5 (*c* 0.2, MeOH); UV (MeCN) λ_{max} (log ε) 276 (3.19) and 350 (2.42) nm; ECD (9.9×10^{-4} mol/L, MeCN) λ_{max} (Δε) 230 (+3.08), 275 (−1.33), 350 (+0.37) nm; IR (KBr) ν_{max} 3255, 2926, 1622, 1585, 1416, 1269, 1073, 1001, and 831 cm^{-1}; ^1H and ^{13}C NMR data see Tables 1 and 2, respectively; HRESIMS *m/z* 325.1784 $[M + Na]^+$ (calcd for $C_{19}H_{26}O_3Na$, 325.1774).

2.3.4. 13β-Acetoxy-3α-hydroxy-ent-atis-16-ene-14-one (euphorane D) (4)

Colorless crystals; mp 145.0–148.6 °C; $[\alpha]_D^{20}$ + 17.5 (*c* 0.4, MeOH); UV (MeCN) λ_{max} (log ε) 203 (3.46) nm; IR (KBr) ν_{max} 3442, 2930, 1746, 1729, 1370, 1230, 1055, 1033, 975, 946, 898, and 735 cm^{-1}; ^1H and ^{13}C NMR data see Tables 1 and 2, respectively; HRESIMS *m/z* 383.2205 $[M + Na]^+$ (calcd for $C_{22}H_{32}O_4Na$, 383.2193).

2.4. ECD and 1D NMR calculations

The structure of **3** was studied by quantum chemical calculation. Details of calculation procedure was provided in the Supplementary Material.

2.5. Crystallographic data

Euphorane A (**1**) was recrystallized in EtOH to give colorless crystals. Euphorane B (**2**) was recrystallized in PE/CH_2Cl_2 (5:1) to give colorless crystals. Euphorane D (**4**) was recrystallized in PE/EtOAc (4:1) to give colorless crystals. (23*E*)-25-methoxycycloart-23-en-3*β*-ol (**11**) was recrystallized in MeOH to afford colorless needles. Their X-ray crystallographic data have been deposited at the Cambridge Crystallographic Data Centre, CCDC Numbers 2184857 (**1**), 2184871 (**2**), 2184873 (**4**), and 2184858 (**11**).

2.5.1. Euphorane A (1)

$C_{20}H_{28}O_3$ (M = 316.42 g/mol): monoclinic, space group $P2_1$ (no. 4), *a* = 10.0198(8) Å, *b* = 7.9319(6) Å, *c* = 10.6903(5) Å, *β* = 97.363(6)°, *V* = 842.62(10) $Å^3$, *Z* = 2, *T* = 100.00 (10) K, μ(Cu Kα) = 0.648 mm^{-1}, *Dcalc* = 1.247 g/cm^3, 16479 reflections measured (8.34° ≤ 2Θ ≤ 157.626°), 3418 unique (R_{int} = 0.1437, R_{sigma} = 0.0824) which were used in all calculations. The final R_1 was 0.0715 (I > 2σ(I)) and wR_2 was 0.1897 (all data). Flack parameter = 0.1(3).

2.5.2. Euphorane B (2)

$C_{17}H_{26}O_3$ (M + H_2O = 278.38 g/mol): monoclinic, space group $P2_1$ (no. 4), *a* = 12.5386(3) Å, *b* = 7.8476(2) Å, *c* = 15.9368(4) Å, *β* = 96.696(2)°, *V* = 1557.45(7) $Å^3$, *Z* = 4, *T* = 99.99(10) K, μ(Cu Kα) = 0.631 mm^{-1}, *Dcalc* = 1.187 g/cm^3, 30,951 reflections measured (5.584° ≤ 2Θ ≤ 154.208°), 6420 unique (R_{int} = 0.1043, R_{sigma} = 0.0721) which were used in all calculations. The final R_1 was 0.0523 (I > 2σ(I)) and wR_2 was 0.1492 (all data). Flack parameter = − 0.11(14).

2.5.3. Euphorane D (4)

$C_{22}H_{32}O_4$ (M = 360.47 g/mol): monoclinic, space group $P2_1$ (no. 4), *a* = 7.42590(10) Å, *b* = 11.16680(10) Å, *c* = 23.2313(3) Å, *β* = 90.0980(10)°, *V* = 1926.42(4) $Å^3$, *Z* = 4, *T* = 99.99(10) K, μ(Cu Kα) = 0.668 mm^{-1}, *Dcalc* = 1.243 g/cm^3, 38,225 reflections measured (3.804° ≤ 2Θ ≤ 144.254°), 6856 unique (R_{int} = 0.0797, R_{sigma} = 0.0561) which were used in all calculations. The final R_1 was 0.0448 (I > 2σ(I)) and wR_2 was 0.1261 (all data). Flack parameter = 0.07(14).

2.5.4. (23E)-25-methoxycycloart-23-en-3β-ol (11)

$C_{31}H_{52}O_2$ (*M* = 456.72 g/mol): monoclinic, space group $P2_1$ (no. 4), *a* = 12.8731(3) Å, *b* = 7.2205(2) Å, *c* = 14.8704(3) Å, *β* = 90.868(2)°, *V* = 1382.05(6) $Å^3$, *Z* = 2, *T* = 100.00 (10) K, μ(Cu Kα) = 0.496 mm^{-1}, *Dcalc* = 1.098 g/cm^3, 27759 reflections measured (5.944° ≤ 2Θ ≤ 158.296°), 5618 unique (R_{int} = 0.1236, R_{sigma} = 0.0701) which were used in all calculations. The final R_1 was 0.0571 (I > 2σ(I)) and wR_2 was 0.1532 (all data). Flack parameter = − 0.1(3).

2.6. Cell culture

The human cancer cell lines HEL (erythroleukemia), K562 (chronic myelogenous leukemia), PC3 (prostatic cancer), MCF-7 (breast cancer), and HepG2 (liver cancer) were obtained from the American Type Culture Collection (ATCC, Manassas, VA, USA) and maintained in RPMI 1640 (HyClone) containing 5 % fetal bovine serum (GIBCO) at 37 °C under a humidified 5 % CO_2 atmosphere.

2.7. Cytotoxicity assay

Cytotoxicity of compounds **1**–**16** against cancer cell line was assessed using MTT method. 5×10^3 Cells per well were seeded into 96-well plates. After 24 h, cells were treated with tested compounds at different concentrations for 72 h. Then, cells were cultured with MTT for 4 h. After removing the supernatant, DMSO was added to dissolve the formazan crystals. The absorbance values were measured at 490 nm. The IC_{50} values of indicated compounds were determined based on the relative survival curves.

2.8. Apoptosis analysis

For apoptosis measurement, K562 cells (5×10^5/well) were seeded into 6-well plates and treated with different concentrations of **3** (4 μM and 8 μM) or DMSO (control) for 24 h and 48 h. After being washed by pre-cooled PBS, cells were double stained using FITC-Annexin V/PI Apoptosis Detection Kit (BD Biosciences, NJ, USA) and analyzed on flow cytometry according to manufacturer guideline.

2.9. Cell cycle analysis

To assess cell cycle, K562 cells (5×10^5/well) were seeded into 6-well plates and treated with different concentrations of **3** (4 μM and 8 μM) or DMSO (control) for 12 h. After being collected and washed with pre-cooled PBS, cells were permeabilized and fixed in paraformaldehyde containing 0.1 % triton X-100. Then, cells were washed twice with pre-cooled PBS, followed by incubation with the mixture of Ribonuclease A (RNaseA, Takara Bio, Beijing, China) and propidium iodide (PI, BD Biosciences, NJ, USA) in the dark for 30 min at 37 °C. Finally, cell cycle was analyzed by FACS Calibur flow cytometer (BD Biosciences, NJ, USA).

3. Results and discussion

The whole plants of *E. dracunculoides* were extracted with 95 % EtOH and then partitioned with EtOAc. The obtained EtOAc extract was separated by various column chromatographic methods to afford compounds **1**–**16** (Fig. 1).

Compound **1** was isolated as colorless needles and showed a molecular formula of $C_{20}H_{28}O_3$ according to the HRESMS at *m/z* 339.1920 $[M + Na]^+$ (calcd for $C_{20}H_{28}O_3Na$, 339.1931). Its IR spectrum displayed the absorptions for hydroxyl (3421 cm^{-1}) and carbonyl (1742 cm^{-1}) groups. The ^1H NMR data (Table 1) of **1** showed signals for four methyls (δ_H 0.86, 0.88, 0.91, and 1.97), two oxygenated methines [δ_H 4.58 (1H, dd, J = 11.8, 6.2 Hz) and 5.05 (1H, s)], an olefinic proton [δ_H 5.99 (1H, s)] and a series of multiplets for aliphatic protons. The ^{13}C NMR data of **1** (Table 2) showed 20 carbon resonances, which was classified as an ester carbonyl (δ_C 174.9), two double bonds (δ_C 123.7, 129.6, 135.8, and 162.3), four sp^3 methines (two oxyganated at δ_C 70.5 and 78.3), five sp^3 methylenes, four methyls, and two sp^3 quaternary carbons (δ_C 32.8 and 36.2). The above NMR data were very similar to those of a reported abietane diterpenoid, fischeriolide A (Lee et al., 2016), except for the replacement of the oxygenated methine (δ_C 65.7, C-11) in fischeriolide A by a methylene (δ_C 27.0) in **1**. This was supported by ^1H–^1H COSY correlations (Fig. 2) from the methylene protons (H_2-11) to H-9 and H-12. Further HMBC and ^1H–^1H COSY analysis confirmed the gross structure of **1**.

The relative configuration of **1** was partially determined by a NOESY experiment. As shown in Fig. 3, the correlations of H-5/H-9 and H_3-20/H-6α indicated that these protons were pseudoaxially oriented on the half-chair conformational B ring. H-5 and H-9 were arbitrarily designated as β-orientation, while CH_3-20 was determined as α-orientation. Thus, the NOESY correlation from H_3-20 to H-12 assigned H-12 to be α-orientation. As the absence of NOESY correlation from H-14 to H-9, the remaining configuration of H-14 was difficult to confirm. Fortunately, a qualified crystal of compound **1** was obtained *via* recrystallization in EtOH, and subsequent X-ray diffraction analysis accurately assigned the absolute configuration of **1** as 5*R*,9*S*,10*R*,12*R*,14*S* (Fig. 4).

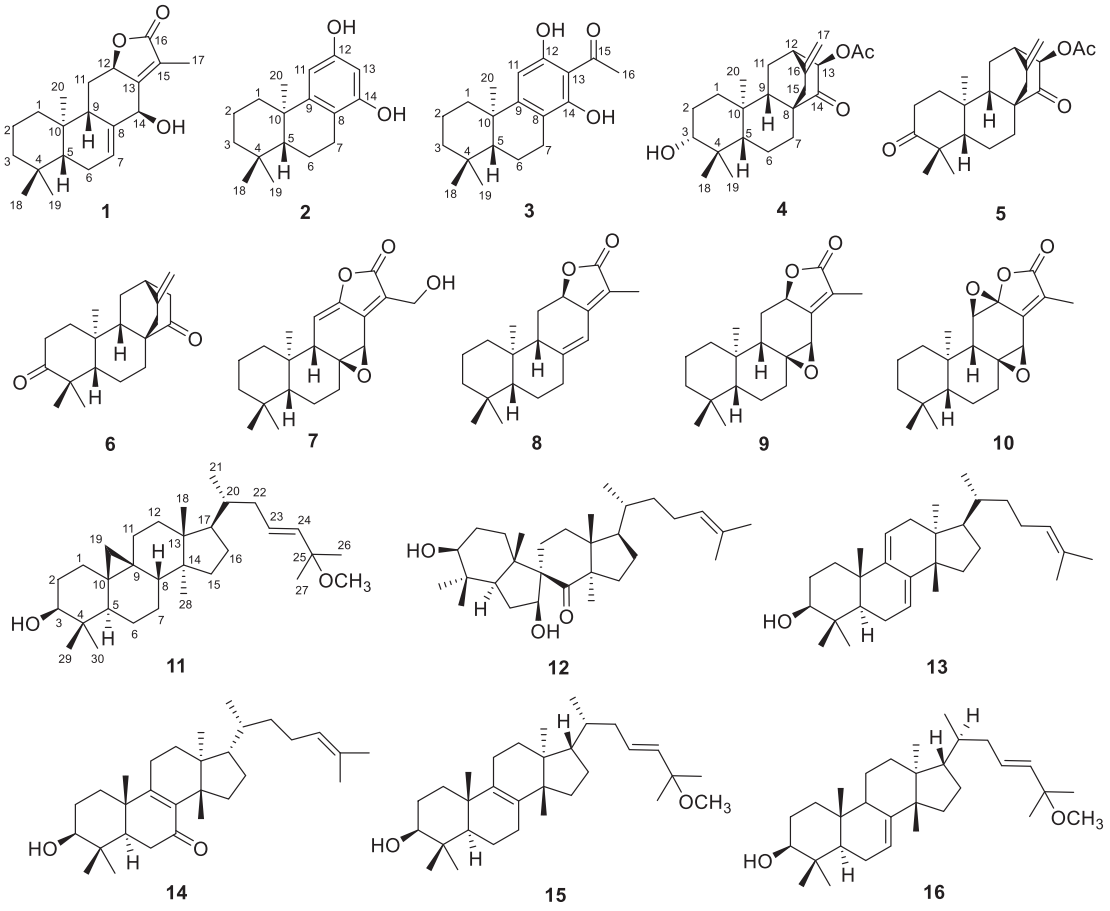

Fig. 1 Structures of compounds **1**–**16**.

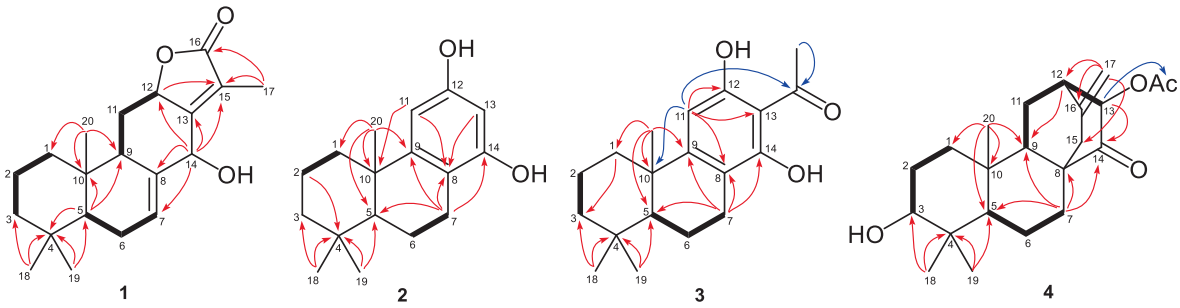

Fig. 2 Key $^{1}H-^{1}H$ COSY (▬) and HMBC (arrows) correlations of **1**–**4**.

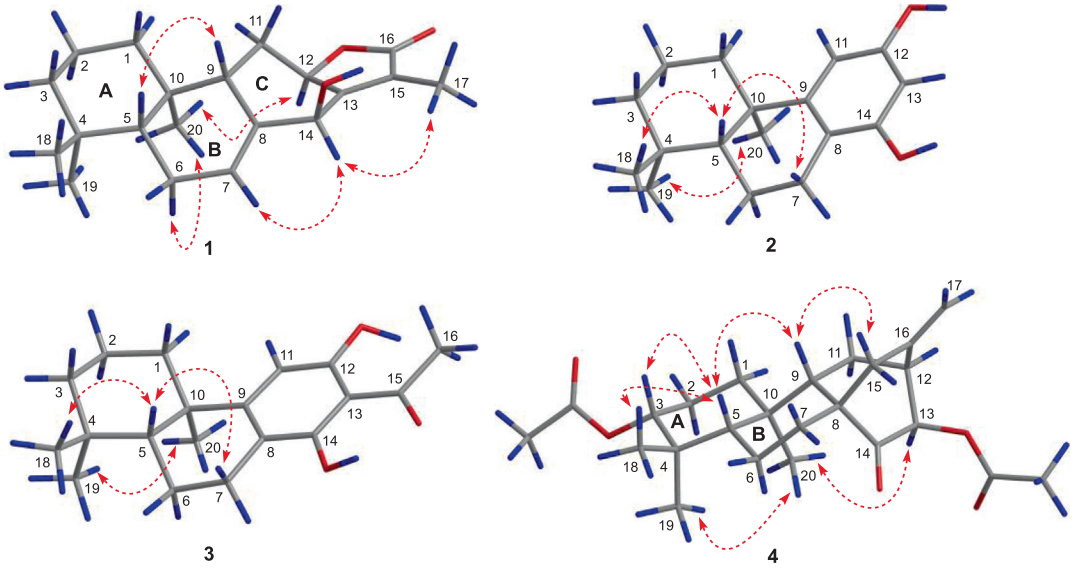

Fig. 3 Key NOESY correlations (◂- - -▸) of **1**–**4**.

Thus, compound **1** was assigned as 14*β*-hydroxy-*ent*-abieta-13 (15)-ene-12*α*,16-olide and was given the trivial name euphorane A.

Compound **2** had a molecular formula of $C_{17}H_{24}O_2$ as determined by the HRESIMS at *m*/*z* 259.1707 $[M - H]^-$ (calcd $C_{17}H_{23}O_2$, 259.1704) and ^{13}C NMR data. The 1D NMR data of **2** were similar to those of a known podocarpane-like trinorditerpene, 7-deoxynimbidiol (Alvarez-manzaneda et al., 2007; Xiong et al., 2006), with the major differences focusing on the ^{13}C chemical shifts in the aromatic ring C (e.g. δ_C 141.2, 141.5, and 143.6 in 7-deoxynimbidiol and δ_C 153.3, 156.4, and 156.4 in **2**), suggesting that the two phenolic hydroxyls in **2** might be at C-12 and C-14 respectively. This was supported by HMBC correlations from an aromatic proton (δ_C 6.25, H-11) to C-10 and C-8, and from another aromatic proton (δ_C 6.10, H-13) to C-8 (Fig. 2). The relative configuration was determined to be the same as that of 7-deoxynimbidiol based on their similar ^{13}C NMR data around rings A and B. This assignment was also supported by the NOESY correlations of H_3-20/H_3-19 and H_3-18/H-5 (Fig. 3). To determine the absolute configuration of **2**, a single crystal X-ray diffraction analysis was conducted, and the results showed that **2** possessed a 5*R*,10*R* configuration (Fig. 4), contrary to that of 7-deoxynimbidiol (5*S*,10*S*). Thus, compound **2** was assigned as an unusual aromatic 15,16,17-trinorabietane diterpenoid and was named euphorane B.

Compound **3** (euphorane C) had a molecular formula of $C_{19}H_{26}O_3$ as determined by its HRESIMS and ^{13}C NMR data. The 1D NMR data of **3** were very similar to those of **2**, except for the absence of signals for an aromatic methine (δ_C 100.3, δ_H 6.10) and the presence of additional signals for an aromatic quaternary carbon (δ_C 109.3) and an ethanone fragment (δ_C 205.9 and 33.9, δ_H 2.95) in **3**, suggesting that **3** was a C-13 acetylated derivative of **2**. Observation of a four-bond W-type HMBC correlation from the aromatic proton (δ_H 6.70, H-11) to the ketone carbonyl (δ_C 205.9) confirmed this assignment. Similar ^{13}C NMR data around the aromatic ring C of **3** and a synthesized analogue **S1** (Fig. 5A) (Shockley et al., 2014) also supported this conclusion. Further computational calculation of the 1D NMR data of two positional isomers **3a** and **3b** (Fig. 5A) by gauge-independent atomic orbital (GIAO) method and analyzed by the improved probability DP4 + method confirmed this structure. As indicated in Fig. 5B, Tables S4 and S5, a final DP4 + probability score of 100.00 % and 0.00 % was obtained for **3b** and **3a** respectively, and the experimental ^{13}C NMR data around ring C in **3** matched well with those calculated for isomer **3b** (Fig. 5A, Table S2, S4). These results indicated that compound **3** had

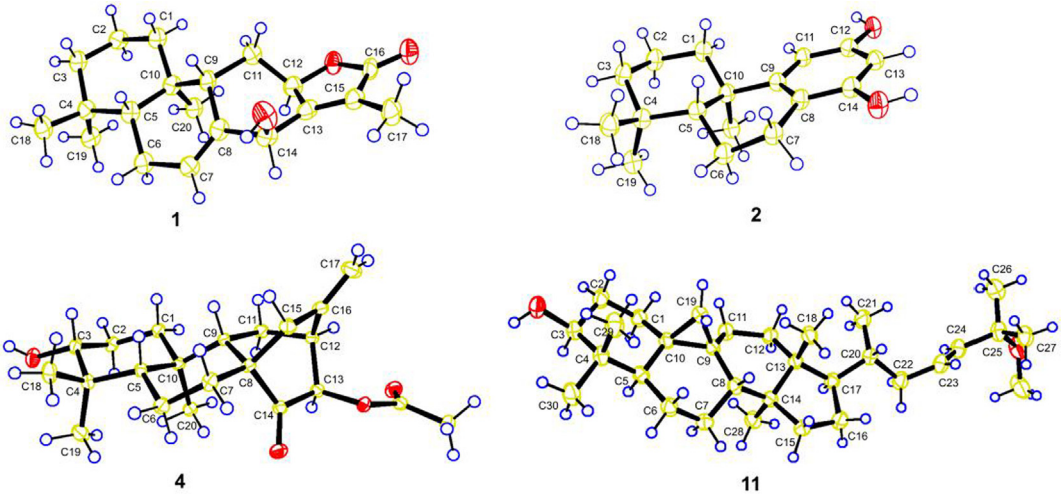

Fig. 4 X-ray structures of compounds **1**, **2**, **4**, and **11**.

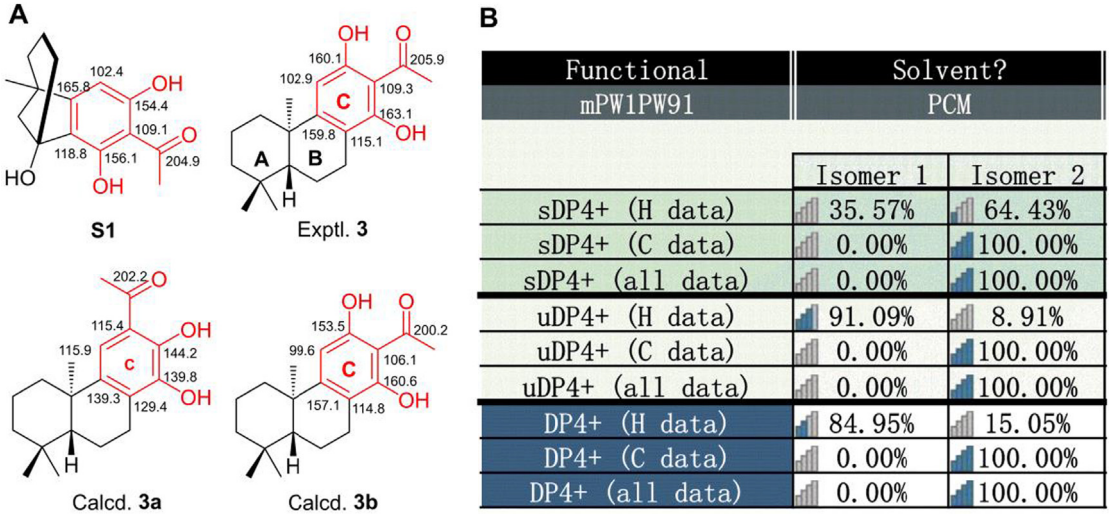

Fig. 5 1D NMR calculation of **3.** (A) Structures of **S1**, **3**, **3a**, and **3b**, and their experimental or calculated ^{13}C NMR data around ring C. (B) DP4 + probability of 1D NMR data of **3a** (isomer 1) and **3b** (isomer 2).

a structure as depicted and was a rare C17-norabietane diterpenoid.

The relative configuration of **3** was determined to be the same as that of **2** based on their similar 1D NMR data around rings A and B. This assignment was also supported by the NOESY correlations of **3** (Fig. 3). Then, the absolute stereochemistry of **3** could be studied by comparison of its experimental and calculated ECD spectra. As shown in Fig. 6, the experimental ECD curve of **3** (**3b**) showed four Cotton effects around 200 (−), 230 (+), 275 (−), and 350 (+) nm respectively, which matched well with those calculated for the isomer **5*R*,10*R*-3b**, indicating that **3** possessed the same absolute configuration (5*R*,10*R*).

Euphorane C (**3**) is an unusual C17-norabietane diterpenoid, and its biosynthetic pathway was proposed in Scheme 1. Briefly, proton-initiated polyene cyclization of *trans*-geranylgeranyl diphosphate could successively produce (+)-copalyl diphosphate and pimarane-like diterpene. Then, 1,2-migration of methyl from C-13 to C-15 constructed the characteristic isopropyl group of the abietane-like precursor, which further underwent the aromatization to give an important intermediate **i** (Ravn et al., 2002; Yang et al., 2002). The hydroxylations of C-12 and C-14 followed by oxidation of CH_3-17 in **i** afforded intermediate **ii**. Finally, the C17-norabietane diterpenoid (**3**) might be generated from **ii** *via* decarboxylization and oxidation reactions (Reis et al., 2014; Wang et al., 2015; Yun et al., 2018).

Compound **4** was isolated as colorless crystals. Its molecular formula was determined as $C_{22}H_{32}O_4$ by the HRESIMS at *m*/*z* 383.2205 $[M + Na]^+$ (calcd for $C_{22}H_{32}O_4Na$, 383.2193). The 1D NMR data of **4** were very similar to those of a reported *ent*-atisane diterpenoid, *ent*-(3*β*,13*S*)-3,13-dihydroxyatis-16-en-14-one (Zhang et al., 2012), except for the presence of an additional acetyl in **4**, suggesting that **4** was an *O*-acetylated derivative of the reported compound. This was supported by its 2D NMR data (Fig. 2), and the ace-

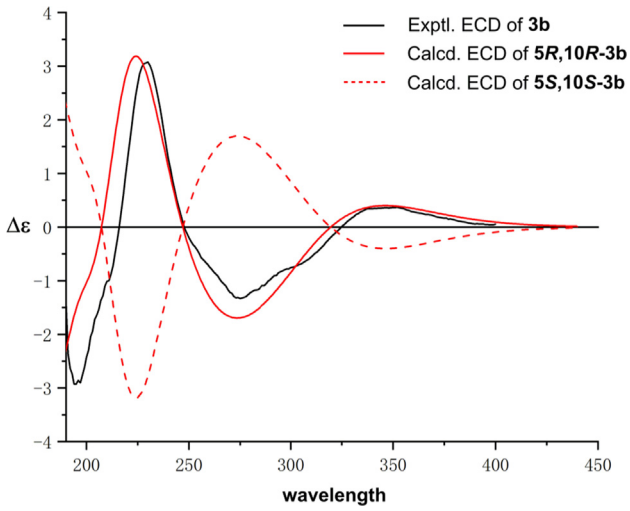

Fig. 6 The experimental and calculated ECD curves of **3**.

toxyl group was located at C-13 by the HMBC correlation from H-13 to the carbonyl (δ_C 170.5). The relative configuration of **4** was determined by the NOESY experiment. As shown in Fig. 3, the NOESY correlations of H-5/H-3, H-5/H_3-18, and H_3-20/H_3-19 suggested that H-5, H-3, CH_3-19, and CH_3-20 occupied the axial positions of the chair conformational A ring. H-3 and H-5 were arbitrarily designated as β-orientations, CH_3-19 and CH_3-20 were accordingly determined as α-orientations. Thus, the NOESY correlations of H-5/H-9 and H-9/H_2-15 established the β-orientation of H-9 and C-8 − C-15, while the NOESY correlation of H_3-20/H-13 assigned H-13 as α-orientation. Furthermore, the absolute stereochemistry of **4** was determined by single crystal X-ray diffraction experiment to be 3*R*,5*S*,8*S*,9*S*,10*R*,12*S*,13*R* (Fig. 4). Thus, compound **4** was assigned as 13β-acetoxy-3α-hydroxy-*ent*-atis-16-ene-14-one and was named euphorane D.

Compound **11** was identified as (23*E*)-25-methoxycycloart-23-en-3β-ol, a known cycloartane triterpenoid, by comparing its 1D NMR data with those reported (Cabrera et al., 1996; Zhang et al., 2005). However, the absolute stereochemistry of **11** remains to be determined. Thus, a recrystallization experiment was carried out, and a qualified crystal of **11** was obtained in MeOH. The crystallographic data exactly assigned the absolute stereochemistry of **11** as 3*S*,5*R*,8*S*,9*S*,10*R*,13*R*,14*S*,17*R*,20*R* (Fig. 4).

Other known compounds, 13-acetyloxy-atis-16-ene-3,14-dione (**5**) (Jia et al., 1990), *ent*-3,14-dioxo-16-atisene (**6**) (Lal et al., 1989), 17-hydroxyjolkinolide A (**7**) (Che et al., 1999), jolkinolide E (**8**) (Lal et al., 1990), jolkinolide A (**9**) (Lal et al., 1990), jolkinolide B (**10**) (Che et al., 1999), spiroinonotsuoxodiol (**12**) (Handa et al., 2010), agnosterol (**13**) (Emmons et al., 1989), kansenone (**14**) (Wang et al., 2003), 3β-hydroxy-25-methyloxylanosta-8,23-diene (**15**) (Fang et al., 2015), and cornusalterin A (**16**) (Kim et al., 2011) were identified by comparison of their NMR data with those reported in the literature.

The antiproliferative activities of compounds **1**–**16** were evaluated on five human cancer cell lines. As shown in Table 3, most of the tested compounds only showed mild to none inhibitory activity against the cancer cells. Compounds **10** and **13** imparted cytotoxicity against the chronic myelogenous leukemia cell line (K562) with IC_{50} values of 7.23 and 5.63 μM respectively. Notably, compound **3** demonstrated significant antiproliferative activity against four of the cancer cell lines with micromolar IC_{50}, and had the highest activity against K562 cells (IC_{50} = 3.59 μM). Thus, the preliminary mechanism of **3** on inhibiting K562 cells was further investigated by using flow cytometry. As shown in Fig. 7, the treatment of **3** at 4 and 8 μM dose- and time-dependently induced apoptosis of K562 cells as compared to the DMSO treated group. Furthermore, we tested whether **3** could arrest cell cycle. The results showed that **3** treatments (4 and 8 μM) changed cell cycle progression as shown by increased G0/G1 and reduced G2/M cell population (Fig. 8), suggesting that **3** arrested K562 cell cycle at G0/G1 phase. Taken together, compound **3** could arrest cell cycle at G0/G1 phase, finally leading to the apoptosis of K562 cells.

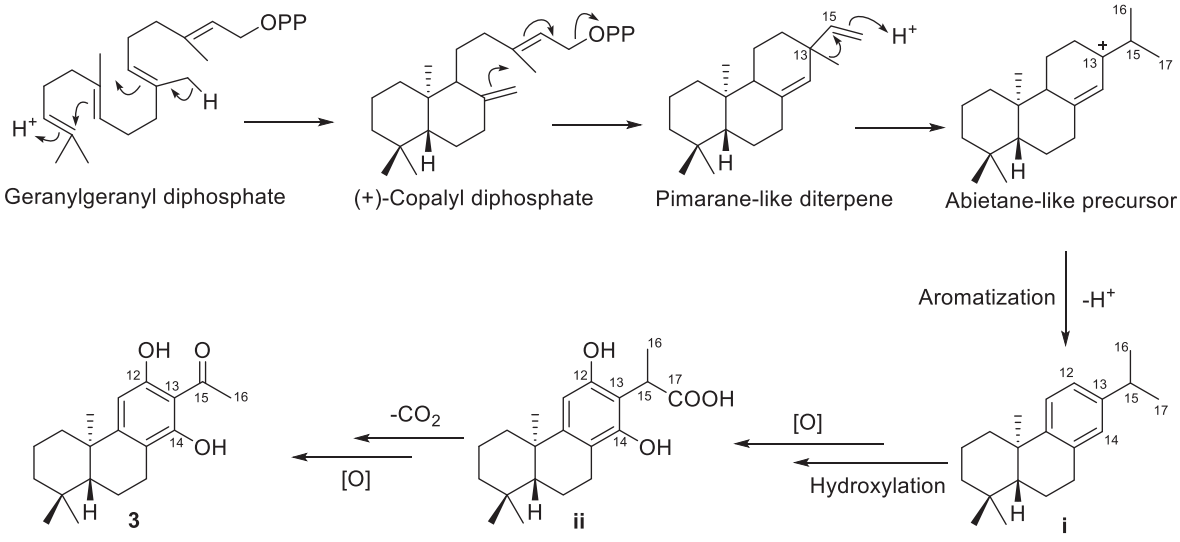

Scheme 1 Proposed Biosynthetic Pathway of **3**.

Table 3 IC_{50}s of compounds **1–16** (μM) for the indicated cell lines.

Compounds	Cell lines				
	MCF7	HEL	PC3	HepG2	K562
1	7.10	> 20	> 20	> 20	21.4
2	20.98	> 20	> 20	> 20	18.23
3	> 20	10.23	10.22	6.95	3.59
4	> 20	> 20	> 20	> 20	> 20
5	> 20	> 20	> 20	> 20	> 20
6	> 20	> 20	> 20	> 20	> 20
7	> 20	9.60	> 20	> 20	17.23
8	> 20	> 20	> 20	> 20	> 20
9	> 20	> 20	> 20	> 20	> 20
10	> 20	10.65	8.76	> 20	7.23
11	> 20	> 20	> 20	> 20	> 20
12	> 20	> 20	> 20	> 20	> 20
13	> 20	16.3	> 20	> 20	5.63
14	> 20	> 20	> 20	> 20	> 20
15	> 20	> 20	> 20	> 20	> 20
16	> 20	> 20	> 20	> 20	> 20
Doxorubicin	1.02	0.42	0.63	1.87	0.96

Doxorubicin is the positive control.

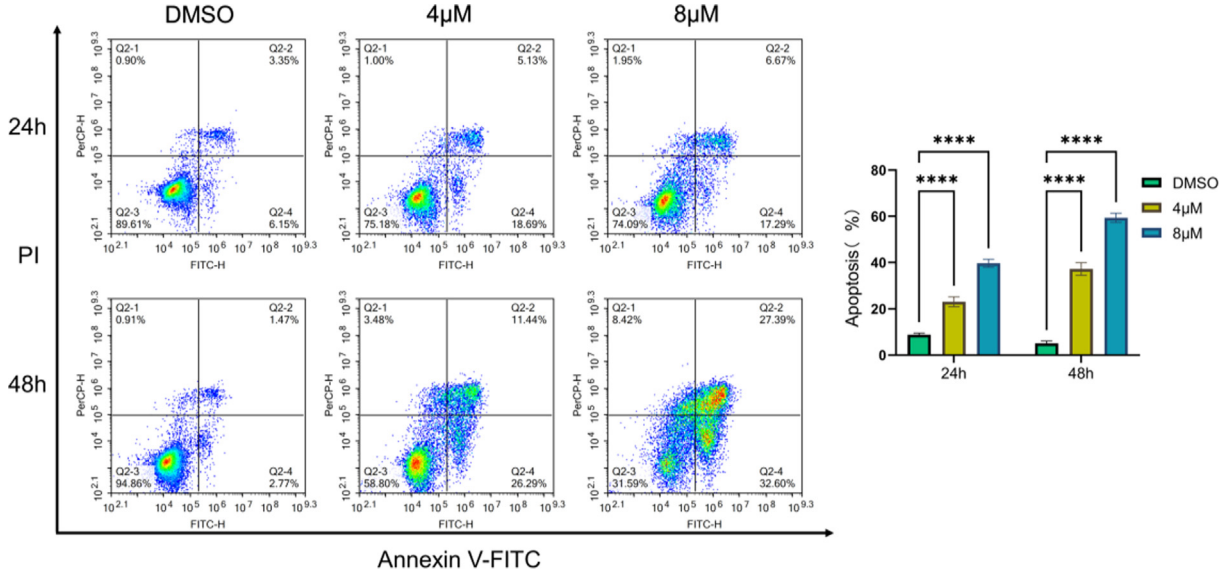

Fig. 7 Compound **3** induced apoptosis of K562 cells**.** The corresponding quantitative analysis was included. Data represented the mean ± SD of at least three independent experiments. ****$P < 0.0001$ vs DMSO treated group.

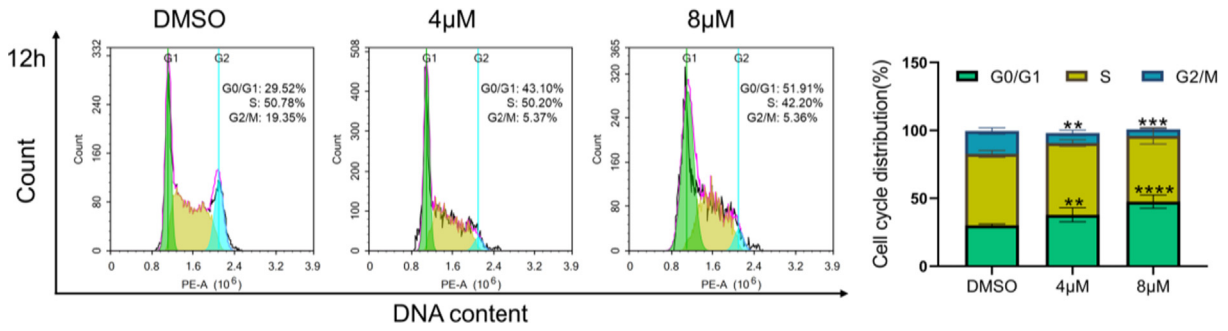

Fig. 8 Compound **3** arrested K562 cell cycle at G0/G1 phase. Quantitative analysis was included. Data represented the mean ± SD of at least three independent experiments. **$P < 0.01$, ***$P < 0.001$ and ****$P < 0.0001$ vs DMSO treated group.

4. Conclusions

Polycyclic diterpenoids, such as abietanes (6/6/6 ring system) with 20α-CH_3 and 5β-H relative configuration, were common natural products in *Euphorbia* species. However, abietane trinor or norditerpenoids were rarely discovered in *Euphorbia* plants (Shi et al., 2008; Vasas et al., 2014; Xu et al., 2021). In the study, chemical investigation of *E. dracunculoides* led to the isolation of four new polycyclic diterpenoids (**1**–**4**) and 12 known terpenoids. Among them, euphorane B (**2**) represents the first example of aromatic 15,16,17-trinorabietane diterpenoid in *Euphorbia* species, while **3** is an unusual 17-norabietane diterpenoid. Biological assay indicated that **3** significantly inhibited the proliferation of K562 cells with micromolar IC_{50}. Preliminary mechanism investigation revealed that **3** could induce cell cycle arrest at G0/G1 phase, causing apoptosis of K562 cells. These findings not only expanded the structural diversity of abietane diterpenoids, but also provided potential chemical scaffold for the development of anti-leukemia drugs. Studies toward the *in vivo* efficacy and in-depth mechanism of **3** are still in progress.

Declaration of Competing Interest

The authors declare that they have no known competing financial interests or personal relationships that could have appeared to influence the work reported in this paper.

Acknowledgements

This work was supported by National Natural Science Foundation of China (22167009), China Postdoctoral Science Fund (2021M693809), Postdoctoral Science Fund of Guizhou Medical University (YJ20073), and the funds from Guizhou Science and Technology Department (Nos. 2020-5006 and 2020-6011).

Appendix A. Supplementary material

Supplementary data to this article can be found online at https://doi.org/10.1016/j.arabjc.2022.104203.

References

Alvarez-Manzaneda, E., Chahboun, R., Cabrera, E., Alvarez, E., Alvarez-Manzaneda, R., Hmamouchi, M., Es-Samti, H., 2007. Novel synthetic strategy toward abietane and podocarpane-type diterpenes from (−)-sclareol: synthesis of the antitumor (+)-7-deoxynimbidiol. Tetrahedron Lett. 48, 8930–8934. https://doi.org/10.1016/j.tetlet.2007.10.080.

Cabrera, G.M., Gallo, M., Seldes, A.M., 1996. Cycloartane derivatives from *Tillandsia usneoides*. J. Nat. Prod. 59, 343–347. https://doi.org/10.1021/np960075+.

Che, C.T., Zhou, T.X., Ma, Q.G., Qin, G.W., Williams, I.D., Wu, H. M., Shi, Z.S., 1999. Diterpenes and aromatic compounds from *Euphorbia fischeriana*. Phytochemistry 52, 117–121. https://doi.org/10.1016/S0031-9422(99)00169-7.

Chen, B.L., Zhu, Q.F., Zhang, X., Lin, Y., Long, Q.D., Liu, W.L., Yan, X.L., 2022. An unusual indole-diterpenoid with C-17 norcassane skeleton from *Euphorbia fischeriana* induces HEL cell cycle arrest and apoptosis. Fitoterapia 159,. https://doi.org/10.1016/j.fitote.2022.105195 105195.

Chi, Y.Q., Wang, L., Ouyang, W.B., Ma, Y.T., Yu, M.M., Zang, Z., Zhao, Y., Huang, S.Q., Zhao, Y., 2016. A new myrinsol diterpenoid ester from *Euphorbia dracunculoides*. Chem. Nat. Compd. 52, 1041–1043. https://doi.org/10.1007/s10600-016-1856-4.

Cragg, G.M., Grothaus, P.G., Newman, D.J., 2009. Impact of natural products on developing new anti-cancer agents. Chem. Rev. 109, 3012–3043. https://doi.org/10.1021/cr900019j.

Dai, L.F., Liang, Q., Liu, T., He, M.Y., Zhao, P., Xu, W.H., 2016. A new tigliane-type diterpene from *Euphorbia dracunculoides* Lam. Nat. Prod. Res. 30, 1639–1645. https://doi.org/10.1080/14786419.2015.1129334.

Emmons, G.T., Wilson, W.K., Schraepfer, G.J., 1989. ^{1}H and ^{13}C NMR assignments for lanostan-3β-ol derivatives: revised assignments for lanosterol. Magn. Reson. Chem. 27, 1012–1024. https://doi.org/10.1002/mrc.1260271103.

Fan, R.Z., Chen, L., Su, T., Li, W., Huang, J.L., Sang, J., Tang, G.H., Yin, S., 2021. Discovery of 8,9-seco-ent-kaurane diterpenoids as potential leads for the treatment of triple-negative breast cancer. J. Med. Chem. 64, 9926–9942. https://doi.org/10.1021/acs.jmedchem.1c00166.

Fang, F.H., Li, W.H., Han, Z.Z., Huang, W.J., Li, D.X., Zhao, S., Tang, M.T., Yuan, C.S., 2015. Terpenoids from *Euphorbia pekinensis*. J. Asian Nat. Prod. Res. 17, 1213–1219. https://doi.org/10.1080/10286020.2015.1118466.

Handa, N., Yamada, T., Tanaka, R., 2010. An unusual lanostane-type triterpenoid, spiroinonotsuoxodiol, and other triterpenoids from *Inonotus obliquus*. Phytochemistry 71, 1774–1779. https://doi.org/10.1016/j.phytochem.2010.07.005.

Jia, Z.J., Ding, Y.L., Wang, Q.G., Liu, Y.T., 1990. Two diterpenes from *Euphorbia sieboldiana*. Phytochemistry 29, 2343–2345. https://doi.org/10.1016/0031-9422(90)83070-H.

Kim, K.H., Choi, S.U., Kim, Y.C., Lee, K.R., 2011. Tirucallane triterpenoids from *Cornus walteri*. J. Nat. Prod. 74, 54–59. https://doi.org/10.1021/np100660v.

Lal, A.R., Camhie, R.C., Rutledge, P.S., Woodgate, P.D., Rickard, C. E.F., Clark, G.R., 1989. New oxidised *ent*-atisene diterpenes from *Eupnorbza fidjiana*. Tetrahedron Lett. 30, 3205–3208. https://doi.org/10.1016/S0040-4039(00)99202-5.

Lal, A.R., Cambie, R.C., Rutledge, P.S., Woodgate, P.D., 1990. *Ent*-pimarane and *ent*-abietane diterpenes from *Euphorbia fidjiana*. Phytochemistry 29, 2239–2246. https://doi.org/10.1016/0031-9422(90)83045-3.

Lee, J.W., Lee, C., Jin, Q., Jang, H., Lee, D., Lee, H.J., Shin, J.W., Han, S.B., Hong, J.T., Kim, Y., Lee, M.K., Hwang, B.Y., 2016. Diterpenoids from the roots of *Euphorbia fischeriana* with inhibitoryeffects on nitric oxide production. J. Nat. Prod. 79, 126–131. https://doi.org/10.1021/acs.jnatprod.5b00789.

Newman, D.J., Cragg, G.M., 2020. Natural products as sources of new drugs over the nearly four decades from 01/1981 to 09/2019. J. Nat. Prod. 83, 770–803. https://doi.org/10.1021/acs.jnatprod.9b01285.

Ravn, M.M., Peters, R.J., Coates, R.M., Croteau, R., 2002. Mechanism of abietadiene synthase catalysis: stereochemistry and stabilization of the cryptic pimarenyl carbocation intermediates. J. Am. Chem. Soc. 124, 6998–7006. https://doi.org/10.1021/ja017734b.

Reis, M.A., Paterna, A., Mónico, A., Molnar, J., Lage, H., Ferreira, M.U., 2014. Diterpenes from *Euphorbia piscatoria*: synergistic interaction of lathyranes with doxorubicin on resistant cancer cells. Planta Med. 80, 1739–1745. https://doi.org/10.1055/s-0034-1383244.

Sang, J., Li, W., Diao, H.J., Fan, R.Z., Huang, J.L., Gan, L., Zou, M. F., Tang, G.H., Yin, S., 2021. Jolkinolide B targets thioredoxin and glutathione systems to induce ROS-mediated paraptosis and apoptosis in bladder cancer cells. Cancer Lett. 509, 13–25. https://doi.org/10.1016/j.canlet.2021.03.030.

Sang, J., Gan, L., Zou, M.F., Lin, Z.J., Fan, R.Z., Huang, J.L., Li, W., Tang, G.H., Yin, S., 2022. Jolkinolide B sensitizes bladder cancer to mTOR inhibitors via dual inhibition of Akt signaling and autophagy. Cancer Lett. 526, 352–362. https://doi.org/10.1016/j.canlet.2021.11.014.

Shi, Q.W., Su, X.H., Kiyota, H., 2008. Chemical and pharmacological research of the plants in genus *Euphorbia*. Chem. Rev. 108, 4295–4327. https://doi.org/10.1021/cr078350s.

Shockley, S.E., Holder, J.C., Stoltz, B.M., 2014. A Catalytic, Enantioselective formal synthesis of (+)-dichroanone and (+)-Taiwaniaquinone H. Org. Lett. 16, 6362–6365. https://doi.org/10.1021/ol5031537.

Vasas, A., Hohmann, J., 2014. *Euphorbia* diterpenes: isolation, structure, biological activity, and synthesis (2008–2012). Chem. Rev. 114, 8579–8612. https://doi.org/10.1021/cr400541j.

Wang, L., Ma, Y.T., Sun, Q.Y., Li, X.N., Yan, Y.J., Yang, J., Yang, F.M., Liu, F.Y., Zang, Z., Wu, X.H., Huang, S.Q., Zhao, Y., 2015a. Structurally diversifified diterpenoids from *Euphorbia dracunculoides*. Tetrahedron 71, 5484–5493. https://doi.org/10.1016/j.tet.2015.06.078.

Wang, L., Ma, Y.T., Sun, Q.Y., Zang, Z., Yang, F.M., Liu, J.P., Jiang, J.H., Huang, S.X., Zhao, Y., 2016. A new lathyrane diterpenoid ester from *Euphorbia dracunculoides*. Chem. Nat. Compd. 52, 1037–1040. https://doi.org/10.1007/s10600-016-1855-5.

Wang, L.Y., Wang, N.L., Yao, X.S., Miyata, S., Kitanaka, S., 2003. Euphane and tirucallane triterpenes from the roots of *Euphorbia kansui* and their in vitro effects on the cell division of *Xenopus*. J. Nat. Prod. 66, 630–633. https://doi.org/10.1021/np0205396.

Wang, L.J., Xiong, J., Liu, S., Pan, L.L., Yang, G.X., Hu, J.F., 2015. ent-Abietane-type and related seco-/nor-diterpenoids from the rare chloranthaceae plant *Chloranthus sessilifolius* and their antineuroinflammatory activities. J. Nat. Prod. 78, 1635–1646. https://doi.org/10.1021/acs.jnatprod.5b00195.

Wang, L., Zang, Z., Wang, Y.F., Huang, S.X., Cao, P., Zhao, Y., 2015b. Two new myrinsol diterpenoids from *Euphorbia dracunculoides* Lam. Chin. Chem. Lett. 26, 121–123. https://doi.org/10.1016/j.cclet.2014.08.005.

Wang, L., Yang, J., Kong, L.M., Deng, J., Xiong, Z.J., Huang, J.P., Luo, J.Y., Yan, Y.J., Hu, Y.K., Li, X.N., Li, Y., Zhao, Y., Huang, S.X., 2017. Natural and Semisynthetic Tigliane Diterpenoids with New Carbon Skeletons from Euphorbia dracunculoides as a Wnt Signaling Pathway Inhibitor. Org. Lett. 19, 3911–3914. https://doi.org/10.1021/acs.orglett.7b01813.

Xiong, Y., Wang, K., Pan, Y.J., Sun, H.X., Tu, J., 2006. Isolation, synthesis, and anti-tumor activities of a novel class of podocarpic diterpenes. Bioorg. Med. Chem. Lett. 16, 786–789. https://doi.org/10.1016/j.bmcl.2005.11.023.

Xu, Y., Tang, P.Y., Zhu, M., Wang, Y.L., Sun, D.J., Li, H., Chen, L. X., 2021. Diterpenoids from the genus *Euphorbia*: structure and biological activity (2013–2019). Phytochemistry 190,. https://doi.org/10.1016/j.phytochem.2021.112846 112846.

Yan, X.L., Zhang, J.S., Huang, J.L., Zhang, Y., Chen, J.Q., Tang, G. H., Yin, S., 2019. Euphonoids A−G, cytotoxic diterpenoids from *Euphorbia fischeriana*. Phytochemistry 166,. https://doi.org/10.1016/j.phytochem.2019.112064 112064.

Yang, J.W., Orihara, Y., 2002. Biosynthesis of abietane diterpenoids in cultured cells of *Torreya nucifera* var. *radicans*: biosynthetic inequality of the FPP part and the terminal IPP. Tetrahedron 58, 1265–1270. https://doi.org/10.1016/S0040-4020(01)01232-7.

Yun, Y.S., Takeda, Y., Fukaya, H., Fuchino, H., Kawahara, N., Takahashi, S., Takahashi, Y., Inoue, H., 2018. A new ent-norabietant diterpenoid from roots of *Euphorbia lathyris* L. Tetrahedron Lett. 59, 2813–2815. https://doi.org/10.1016/j.tetlet.2018.06.017.

Zhang, B.Y., Wang, H., Luo, X.D., Du, Z.Z., Shen, J.W., Wu, H.F., Zhang, X.F., 2012. Bisyinshanic acids A and B, two novel diterpene dimers from the roots of *Euphorbia yinshanica*. Helv. Chim. Acta 95, 1672–1679. https://doi.org/10.1002/hlca.201200092.

Zhang, W.H., Zhong, H.M., Che, C.T., 2005. Cycloartanes from the red alga *Galaxaura* sp. J. Asian Nat. Prod. Res. 7, 59–65. https://doi.org/10.1080/10286020310001617138.